Journal of Information Systems Engineering and Management
2025, 10 (29s)
e-ISSN: 2468-4376
https://jisem-journal.com/

Research Article

An ANFIS Based Grid Connected Renewable Source Bidirectional SEPIC Converter Multifunctional EV Charger With Reduced Peak and Disturbances

P. Vinay Kumar[1], P. Venkata Prasad[2], E. Vidya Sagar[3]

[1]Research Scholar, Department of Electrical Engineering, University College of Engineering (A), Osmania University, Hyderabad, India.

[2] Professors and COE, Department of Electrical and Electronics Engineering Department, CBIT, Hyderabad Telangana, India.

[3] Professor and Head of the Department, Department of Electrical Engineering, University College of Engineering (A), Osmania university, Hyderabad, India.

[1]vinayperumandla@gmail.com

ARTICLE INFO

Received: 20 Dec 2024

Revised: 21 Feb 2025

Accepted: 27 Feb 2025

ABSTRACT

Integration of EV charging modules into the grid is increasing in present day as the utilization of EVs are on rise. At present technology most of the charging stations are unidirectional which only charge the EV battery. In future there might be a requirement of bidirectional converters which have the capability if G2V and V2G operations. In this paper a multifunctional EV charger with bidirectional SEPIC converter and full bridge converter is proposed. The bidirectional charger is included with PV array for renewable power sharing either to the EV battery or to the grid. The bidirectional SEPIC converter is controlled by a G2V/V2G controller with feedback from the DC link voltage and battery measurements. The full bridge converter control is included with SMC voltage regulator which controls current direction between the EV charger and grid. The conventional SMC is replaced with ANFIS current regulator trained using 'back propagation' optimization technique. With this updated to the full bridge controller the peak overshoots of the currents and disturbances during transitions are mitigated to a greater extent. Along with the reduced disturbances the PV array power extraction is also improved. A comparative analysis between the SMC and ANFIS regulator models is presented in this paper using MATLAB Simulink Electrical tools.

Keywords: EV (Electric Vehicle), G2V (Grid to Vehicle), V2G (Vehicle to Grid), SEPIC, PV (Photo Voltaic), SMC (Sliding Mode Control), ANFIS (Adaptive Neuro Fuzzy Inference System), MATLAB Simulink.

1. INTRODUCTION

With the increasing global warming there is drastic raise in climatic disasters creating unreliable conditions for the survival of living beings. The main cause of raising temperatures throughout the globe is transportation pollution produced by the IC (Internal Combustion) engine vehicles. These IC engine vehicles use fossil fuels (petrol or diesel) for driving the vehicle which generates hazardous carbon gases polluting the environment. To reduce the effect of these vehicles on the environment they need to be replaced with zero carbon emission vehicles [1]. This can only be achieved by EVs integrated with battery packs driving the vehicle. As the EV is driven using electrical motor by the battery power there is zero carbon emission from the vehicle [2] [3].

In this paper a multifunctional EV charger is proposed with bidirectional SEPIC converter charging and discharging the battery pack [4]. The bidirectional SEPIC converter is an advanced converter with reduced power loss and stable voltage generation. This converter is interconnected to the grid through a single-phase full bridge for exchange of EV battery power. Along with the bidirectional SEPIC

converter EV battery charging module, a PV array boost converter topology is also connected at the DC link for renewable power sharing [4]. With the PV array connection, the EV battery receives charging power either from PV array or grid. During excess PV power condition, the EV battery is charged by the renewable solar power and the remaining power is shared to the grid. And during deficit PV power condition, the EV battery is charged by both grid and renewable solar power [5]. This is controlled by the full bridge converter control with feedback from the grid and load voltages and currents measurements. The outline structure of the proposed multifunctional SEPIC based EV charging station with renewable power interconnection to the grid is presented in figure 1.

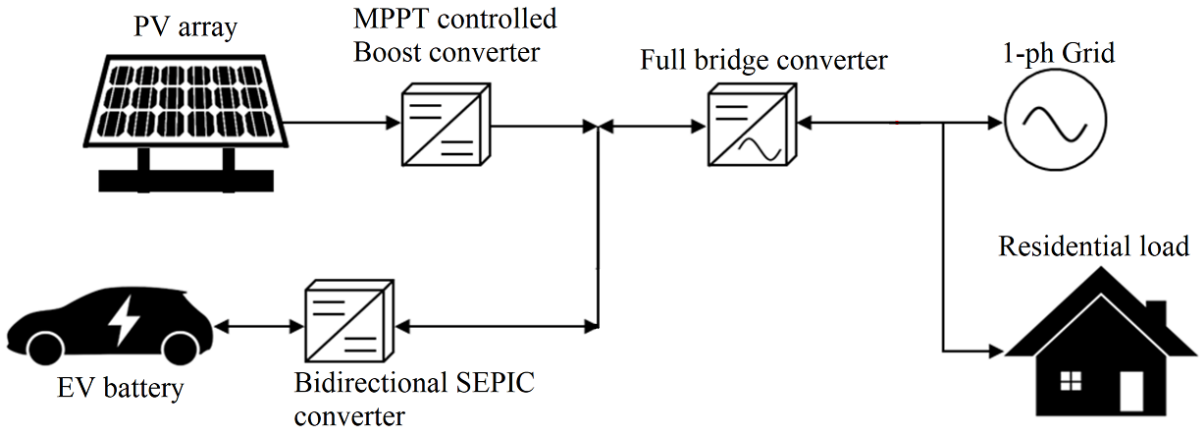

Figure 1: Proposed outline structure of multifunctional EV charging station

As observed in figure 1 the PV array is connected at the DC link through a DC/DC boost converter which is controlled by MPPT (Maximum Power point tracking) technique. The MPPT technique adopted is P&O (Perturb and Observe) technique which takes feedback from the PV array voltage and current for controlling the switch of the boost converter. The converter extracts all the power from the PV array in any solar irradiation condition. The power from the PV array is shared either to the EV charger module or to the grid as per the PV power generated and EV demand [6]. At the same DC link the bidirectional SEPIC converter is also connected which exchanges power between the EV battery and grid. The power exchange between the EV charger module and the grid is carried out through the full bridge converter with 4 IGBTs. The full bridge is controlled by a central control with feedback from residential load current (IL), inverter voltage (Vs) and grid phase angle (θ) to ensure synchronization to the grid.

The EV module operates in two modes (G2V/V2G) with respect to the grid availability. During grid connection the EV module operates on G2V mode which charges from both PV power and grid power. During G2V mode when the PV power is excess than the EV module demand, the remaining power is injected to the grid through the full bridge converter. And when the grid is isolated the as per the PV power the EV module operates in G2V/V2G mode [6]. During grid isolation condition when the PV power is very high which can compensate the residential load, the remaining power is diverted to EV module charging the battery. And when the PV power is less than the residential load demands the EV module operates in V2G mode supporting the load along with PV power. The full bridge converter control is updated with ANFIS voltage regulator replacing SMC regulator for reduced disturbances and peak value generation in the system [7].

This paper is arranged with introduction to the proposed SEPIC converter multifunctional EV charger system with grid and PV array interconnection in section 1. The section 2 is included with the configuration of the proposed system circuit topologies and the control structure designs of the full bridge and bidirectional SEPIC converters. The section 2 is followed by section 3 which includes the modeling of ANFIS voltage regulator and the training procedure tuning the regulator. The section 4 has the results of the simulation carried out on the proposed system with SMC and ANFIS voltage regulators creating comparative results. The validation of the optimal system with reduced disturbances and overshoot is presented in section 5 conclusion to the paper followed by references cited in the paper.

2. PROPOSED SYSTEM CONFIGURATION

The system introduce in the paper has four modules which are PV module, EV module, full bridge inverter module and grid. All these four modules are interconnected through multiple power electronic circuits for exchange of power between them. These circuits are used to convert DC/AC or DC/DC conversion for different voltage levels in order to maintain synchronization between the modules. Each module has its own significance which either delivers or store power as per the operating conditions [8]. The complete circuit structure of the proposed system with all the modules interconnected to each other can be observed in figure 2.

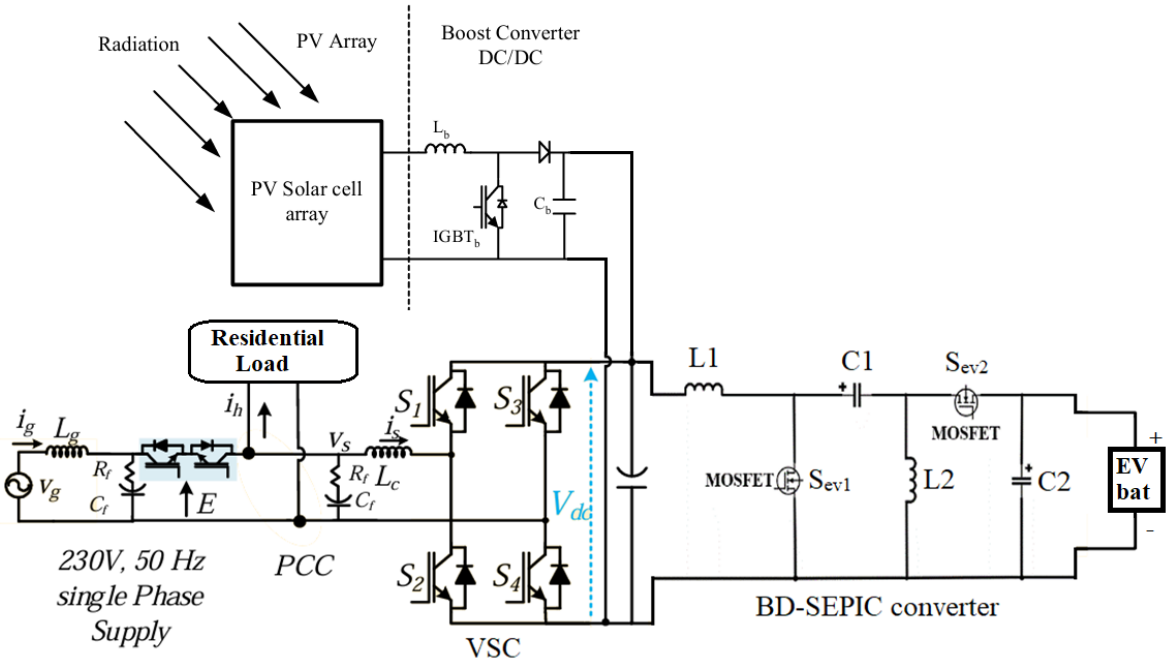

Figure 2: Proposed system circuit configuration

As in figure 2, PV array is connected to a unidirectional boost converter which only extracts power from PV array and delivers to the DC link. From the DC link the PV power might charge the EV battery through bidirectional SEPIC converter or delivered to residential load on the AC side through full bridge converter. The excess power from the PV array will be injected to the grid after compensating the EV battery and residential load demand. The EV battery is connected to the bidirectional SEPIC converter which either charges or discharges the battery using PV array and grid powers.

The input terminals of the SEPIC converter are connected at the DC link where the full bridge converter DC terminals are also connected. The grid is connected to the full bridge converter through LC filter for harmonic mitigation sharing power to the SEPIC converter. The grid isolation is achieved using back-to-back connected IGBT switches after the grid filter. The IGBTs are operated as per the trigger signal 'E' (E=1 - grid connected; E=0 - grid isolation). At the PCC on the AC side a residential load is connected which is either compensated by grid or PV power or EV battery power [9]. Here the residential load is considered to be a critical load which always needs to be compensated irrespective of any operating condition.

A. Bidirectional SEPIC converter design and control

The bidirectional SEPIC converter is an advancement to the conventional bidirectional converter which has reduced ripple and disturbances in voltages and currents [10]. The bidirectional SEPIC converter has two energy storage inductors L_1 L_2, one intermediate capacitor C_1 and one DC capacitor C_2. The passive elements values of the bidirectional SEPIC converter are given as:

$$L_1 = \frac{1}{\eta f_s}\left(\frac{V_{in}^2}{P_{max}}\right)\left(\frac{V_{dc}}{V_{in}+V_{dc}}\right) \quad (1)$$

$$L_2 = \frac{V_{dc}}{2V_{in}f_s}\left(\frac{V_{in}^2}{P_{max}}\right)\left(\frac{V_{dc}}{V_{in}+V_{dc}}\right) \quad (2)$$

$$C_1 = \frac{P_{in}}{\kappa f_s(V_{in}+V_{dc})^2} \quad (3)$$

$$C_2 = \frac{P_{in}}{2\omega\delta V_{dc}^2} \quad (4)$$

Here, V_{in} is the voltage at the DC link, V_{dc} is battery voltage, P_{max} is the maximum power delivered, η is the ripple current percentage, f_s is the switching frequency, P_{in} is the input power, κ ripple voltage percentage, ω is the grid angular frequency and δ is the percentage of output voltage ripple tolerance [11]. The two MOSFET switches S_{ev1} and S_{ev2} are the charge control switches operate complementarily. As per the duty ratio of the switches S_{ev1} and S_{ev2} the direction of power flow is controlled which operates the EV module in G2V/V2G mode [12]. The controller for the bidirectional SEPIC converter switches is presented in figure 3.

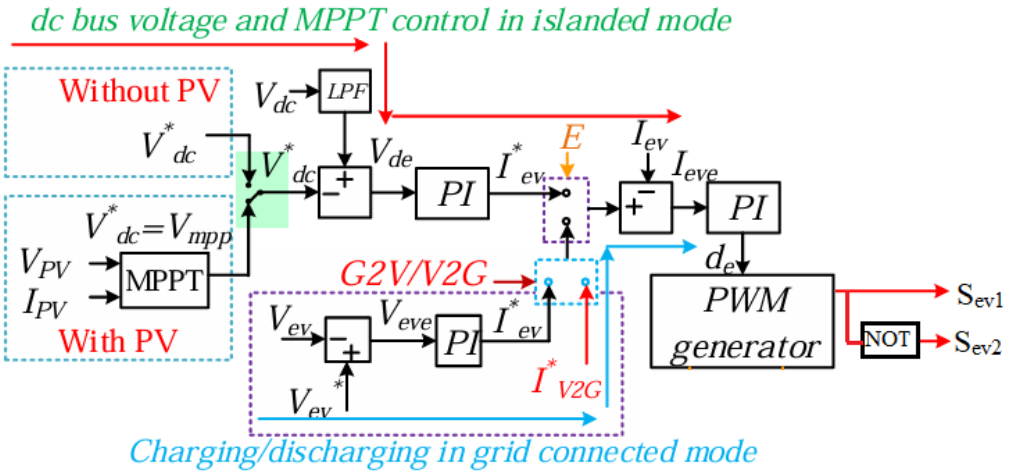

Figure 3: Bidirectional SEPIC converter control

The duty ratio (d_{Sev1}) for the switch S_{ev1} is expressed as:

$$d_{Sev1} = (I^*_{ev} - I_{ev})\left(K_{pd} + \frac{K_{id}}{s}\right) \quad (5)$$

Here, I_{ev} is the EV battery measured current, K_{pd} K_{id} are the proportional and integral gains of the current regulator and I^*_{ev} is the reference EV battery current (during grid isolated mode) with E = 0 is expressed as:

$$I^*_{ev} = (V^*_{dc} - V_{dc})\left(K_p + \frac{K_i}{s}\right) \quad (6)$$

Here, V_{dc} is the measured DC link voltage, K_p K_i are the voltage regulator proportional and integral gains. The V^*_{dc} is the reference DC link voltage determined by the PV array availability given as:

$$V^*_{dc} = \begin{cases} 400; without\ PV\ array \\ V_{mpp}; with\ PV\ array \end{cases} \quad (7)$$

The V_{mpp} is the voltage at maximum power point generated by the P&O MPPT technique. The I^*_{ev} is switched as per the grid availability. If the grid is available with E = 1 the reference current is expressed as:

$$I^*_{ev} = (V^*_{ev} - V_{ev})\left(K_p + \frac{K_i}{s}\right) \quad (8)$$

Here, V_{ev} is measured EV battery voltage and V^*_{ev} is the reference EV battery voltage. The expression is selected for G2V (Charging mode) which charges either from grid or PV array [13]. For the V2G condition the I^*_{ev} is manually set as per the requirement of the system which discharges the EV battery as per the given value.

B. Full bridge converter control

The full bridge converter comprises of four IGBT switches S1-S4 which are operated either by hysteresis current loop or Sinusoidal PWM technique. The two switches S1 S4 and S2 S3 operate simultaneously converting either DC-AC or AC-DC with respect the power flow direction. The full bridge converter operates as a rectifier when the EV battery needs power to charge from the grid. The same converter operates as inverter when the power from either PV array or EV battery needs to be shared to the grid or residential load on the AC side. The full bridge converter operates with hysteresis current loop technique during grid connection and operates with Sinusoidal PWM during grid isolation [14]. The switching between the techniques is done by the grid switch signal 'E'. The complete structure of full bridge converter control is presented in figure 4.

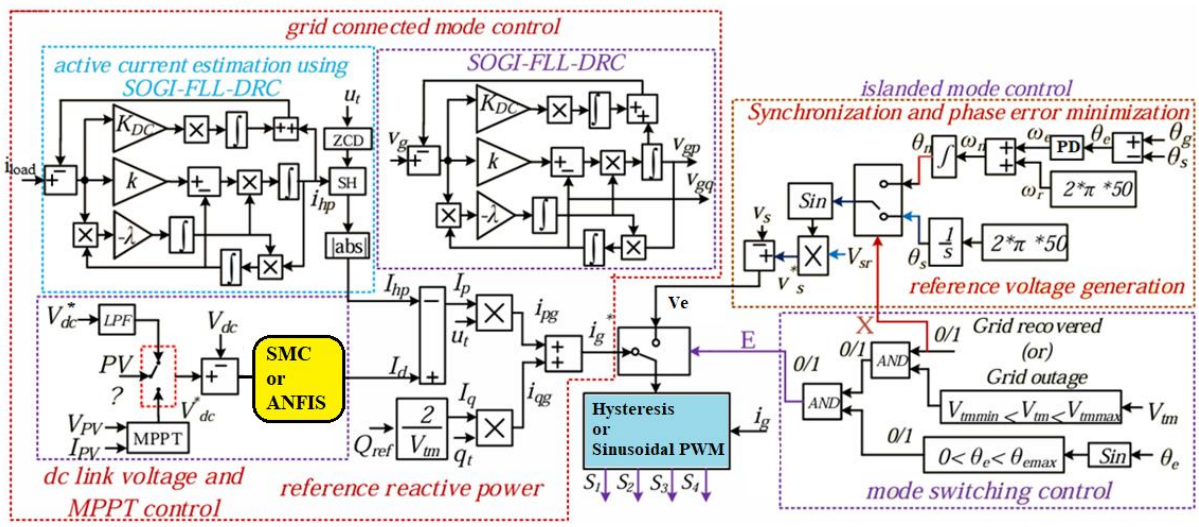

Figure 4: Full bridge converter control structure

In the given control structure, the i_g^* and i_g current components are considered for hysteresis current loop technique during grid connected mode. And the reference error voltage signal (Ve) is considered for Sinusoidal PWM technique during grid isolation mode [15]. The reference signal during grid islanding mode for the Sinusoidal PWM technique is given as:

$$V_e = V_s^* - V_s \tag{9}$$

Here, V_s^* and V_s are the reference inverter voltage signal and measured inverter voltage. The V_s^* signal is expressed as:

$$V_s^* = V_{sr}\, Sin(\theta) \tag{10}$$

Here, θ is the estimated phase angle of the inverter voltage generated by the integration reference angular frequency (w_n). For the grid connected mode the reference current signal for the hysteresis current loop technique is expressed as:

$$i_g^* = i_{pg} + i_{qg} \tag{11}$$

$$i_{pg} = I_p u_t;\ i_{qg} = I_q q_t \tag{12}$$

$$u_t = \frac{v_{gp}}{V_{tm}};\ q_t = \frac{v_{gq}}{V_{tm}} \tag{13}$$

$$V_{tm} = \sqrt{v_{gp}^2 + v_{gq}^2} \tag{14}$$

$$I_p = I_d - I_{hp};\ I_q = Q_{ref}\frac{2}{V_{tm}} \tag{15}$$

In the given expressions (11) – (15), i_{pg} i_{qg} are the active and reactive grid current components, I_p I_q are the load active and reactive current components, u_t q_t are the active and reactive unit vector

templates, v_{gp} v_{gq} are active and reactive grid voltage components generated by SOGI-FLL-DRC module and V_{tm} is the RMS of the v_{gp} v_{gq} components [16]. The I_p value is calculated by the direct axis current I_d component and load voltage magnitude I_{hp}. The I_d value is expressed as:

$$I_d = C_{dc}V_{dc}\left[\left(\frac{1}{R_L C_{dc}} - \frac{1}{\gamma}\right)V_{dc} + \frac{1}{\gamma}V_{dc}^* - (\sigma + \delta)sing(S)\right] \quad (16)$$

Here, C_{dc} capacitance of the capacitor at the DC link, V_{dc} is the voltage across DC link, R_L is the residential load resistance, γ is sliding ratio, σ and δ are sliding coefficients for the SMC the S is the sliding component expressed as:

$$S = \gamma(V_{dc}^* - V_{dc}) + \int(V_{dc}^* - V_{dc})dt \quad (17)$$

The I_d component generated by the SMC module has more disturbances and damping which causes disturbances and overshoots in the system [17]. This SMC is replaced with advanced regulator with optimization technique trained fuzzy system for reduced disturbances and overshoots in the voltages and current of the module connected in the system.

3. ANFIS DESIGN

Adaptive fuzzy control is considered to be an advancement to the SMC regulator as the controller is trained using optimization algorithm from the data generated by the SMC input and output. Therefore, all the demerits of the SMC are overcome by the ANFIS training leading to better results [18]. The ANFIS regulator also takes input from the DC link voltage comparison with reference set value. However, the ANFIS regulator is very much less complex as compared to the SMC (which includes many factors like γ σ δ). The ANFIS structure has only one input variable ($V_{dcerror}$) and one output variable (Id) used for I_p calculation. Each variable comprises of seven membership functions (MFs) set with specific ranges as per the required results. The MFs design of the proposed ANFIS regulator is presented in figure 5.

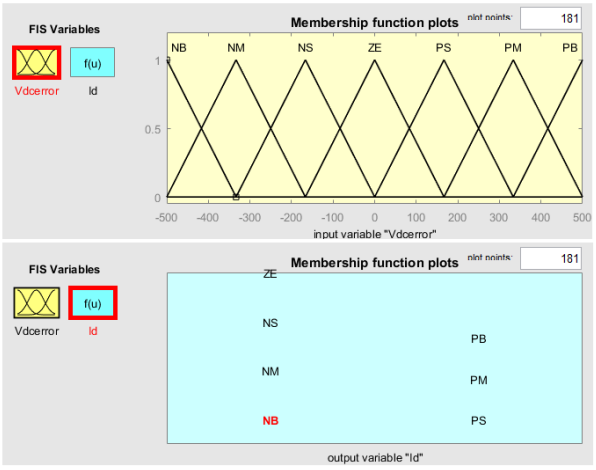

Figure 5: ANFIS MFs design

As presented in figure 5, each MF is named with respect to the placement of the MF position in the range of -500 to 500. The range of the input variable is considered as per the maximum and minimum possible input value. The negative most MF is named as NB (Negative Big) with large negative value, medium range negative is NM (Negative Medium), lower negative is NS (Negative Small). The ZE (Zero) is the center to the native and positive region covering half negative and half positive range. The positive side high value MF is named as PB (Positive Big), medium positive range as PM (Positive Medium) and smaller positive range MF as PS (Positive Small) [19].

The output MFs are set with specific constant value in certain range of -150 to 150 determined by the response of the system to the variable conditions [20]. The rules of the ANFIS design are included in linearization with each input MF linearly ruled to output MF. The rules for the proposed ANFIS regulator are:

1) IF '$V_{dcerror}$' is in 'NB' THEN 'Id' is in 'NB'
2) IF '$V_{dcerror}$' is in 'NM' THEN 'Id' is in 'NM'
3) IF '$V_{dcerror}$' is in 'NS' THEN 'Id' is in 'NS'
4) IF '$V_{dcerror}$' is in 'ZE' THEN 'Id' is in 'ZE'
5) IF '$V_{dcerror}$' is in 'PS' THEN 'Id' is in 'PS'
6) IF '$V_{dcerror}$' is in 'PM' THEN 'Id' is in 'PM'
7) IF '$V_{dcerror}$' is in 'PB' THEN 'Id' is in 'PB'

As per the these seven rules the output is generated after trained from the input and output ($V_{dcerror}$ and Id) data of the SMC. The data from the SMC is used for training the ANFIS MFs with 'back propagation' optimization technique using 100epchos in the tool [21]. The 'imported data' and the 'trained data' by the optimization technique of ANFIS tool is presented in figure 6.

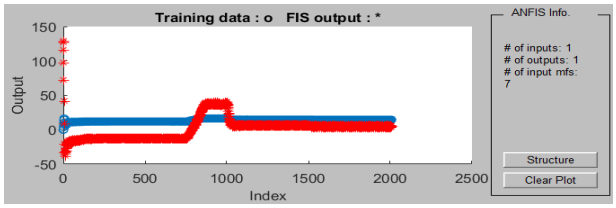

Figure 6: Imported and trained data in ANFIS training tool

As observed in figure 6 the scattered data imported from the SMC regulator is suppressed to a specific range by the optimization technique. As per the new restricted and trained data of the ANFIS MFs the ANFIS regulator is exported to the full bridge control. The simulation for the same changes and rating of the module is carried out and a comparative analysis is presented in followed section.

4. RESULT ANALYSIS

The given proposed system with bidirectional SEPIC multifunctional EV charger connected to grid along with PV array renewable source is modeled in MATLAB Simulink environment. All the blocks from 'Specialized Technology' of the 'Power systems' block set in the Simulink library browser are considered for the modeling. For the controller modeling blocks from 'Math Operations' and 'Commonly used blocks' are used. Two models are compared with two different voltage regulators (SMC and ANFIS) set in the full bridge converter control for the generation of Id signal in the controller. A comparative analysis is presented with graphical overlap plotting determining the optimal operating regulator for the given operating variations. The table 1 is the configuration parameters set into the models maintaining same rating and operating conditions.

Table 1: System configuration parameters

Name of the module	**Parameters**
Grid	1-ph 230V_{rms} 50Hz, L_g = 1mH, C_f = 100µF, Load = 2kW
PV module	Manufacturer: 1Soltech 1STH-350-WH V_{mp} = 43V, I_{mp} = 8.13A, V_{oc} = 51.5V, I_{sc} = 9.4A, N_p = 1, N_s = 10, P_{pv} = 3.5kW Boost converter: L_b = 1mH, C_{pv} = 1000µF, R_{igbt} = 1mΩ.
EV module	Battery pack: V_{nom} = 240V, Capacity = 35Ah Conventional DC/DC converter: L_{bb} = 2.6mH, C_{bb} = 1000µF, R_{igbt} = 1mΩ, f_s = 20kHz
SMC	C_{dc} = 2200µF, $\gamma = 0.1, \sigma = 0.2, \delta = 1.5$, Kdc = 0.01, k =1.414, λ = 49298, f_c = 5kHz
Bidirectional SEPIC	L_1 = L_2 = 2.5mH, C_1 = 80.7µF, C_2 = 1000µF, R_{mosfet} = 0.1Ω, f_s = 20kHz.
ANFIS	Input MFs = 7 (triangular), Input Range = - 500 to 500 Output MFs = 7 (Constant) Output range = -150 to 150

With the above system parameters of the modules set in the models and the ANFIS tool the simulations are carried out. The simulation is set with variable solar irradiation and grid isolation conditions in a simulation time of 2sec. The solar irradiation is dropped to 500W/mt² at 0.75sec which was initially at 1000W/mt² from 0sec. The value of the irradiation is increased back to 700W/mt² at 1.5sec. This variation in the solar irradiation changes the power generated by the PV array impacting the EV module and grid powers. Along with solar irradiation variations the grid is isolated at 1sec changing the 'E' signal from '1' to '0' switching OFF the back-to-back IGBT switches. The graphs of the voltages, currents and powers of all the modules with these conditions are presented below.

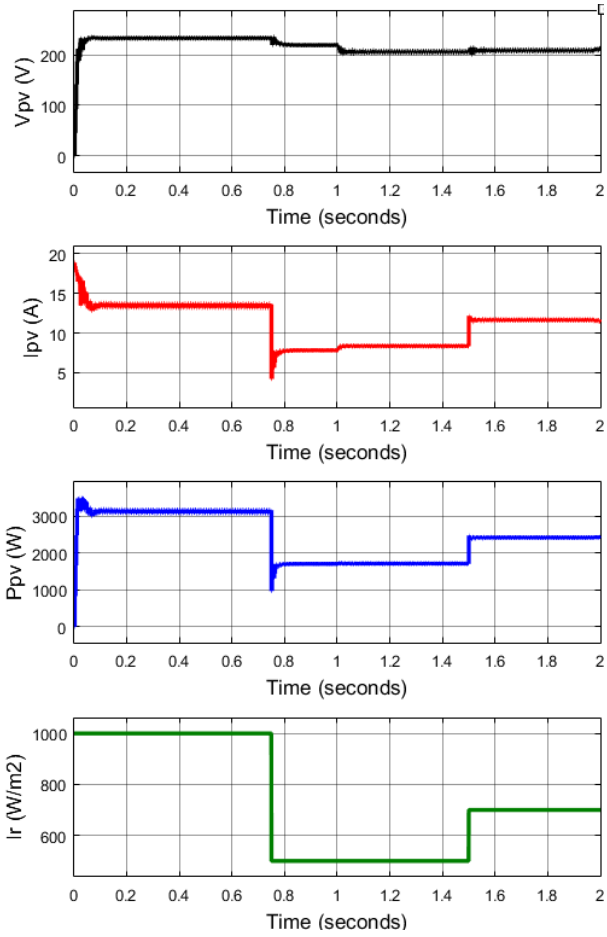

Figure 7: PV array characteristics

The figure 7 represents the graphs of PV array characteristics (voltage, current, power and irradiation). The voltage of the PV array is maintained between 220 – 200V, PV current changes from 14A to 8A to 12A as per the change in solar irradiation. As per these changes the PV power generation is varied which impacts the grid power and EV battery power.

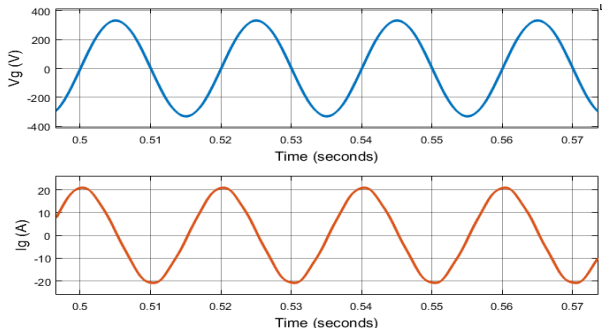

Figure 8: Grid voltage and current

In figure 8 graphs of grid voltage and current are presented which are Sinusoidal recording 325V and 20A maximum values of voltage and current respectively.

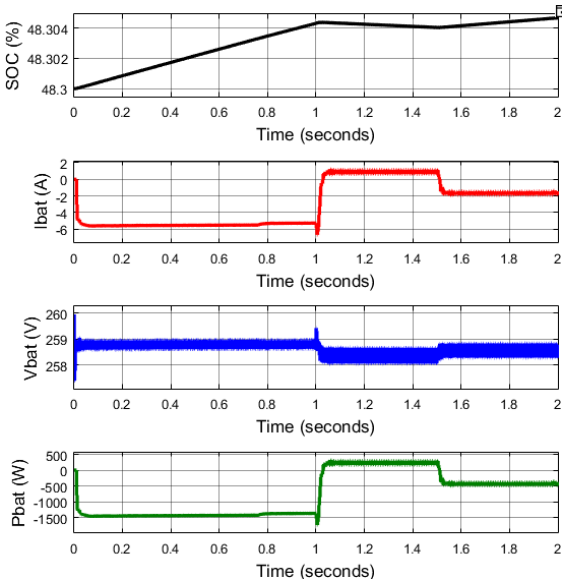

Figure 9: EV battery characteristics

As per changes in the solar irradiation and grid connection, the EV battery characteristics (State of Charge (SOC), current, voltage and power) are presented in figure 9. The SOC raises from 0-1sec when the grid is available and drops from 1-1.5sec when the grid is disconnected due to power deficit condition. From 1.5-2sec the SOC raises again as the PV power is excess after load compensation. With respect to the changes the battery current direction changes from negative to positive regions. However, in any condition the battery voltage is stable at 258V. From 0-1.5sec the battery stores 1.5kW of power with 5.8A charge current, 1-1.5sec battery discharges 200W with 1A discharge current and from 1.5-2sec it charges by 0.5kW with 2A charge current.

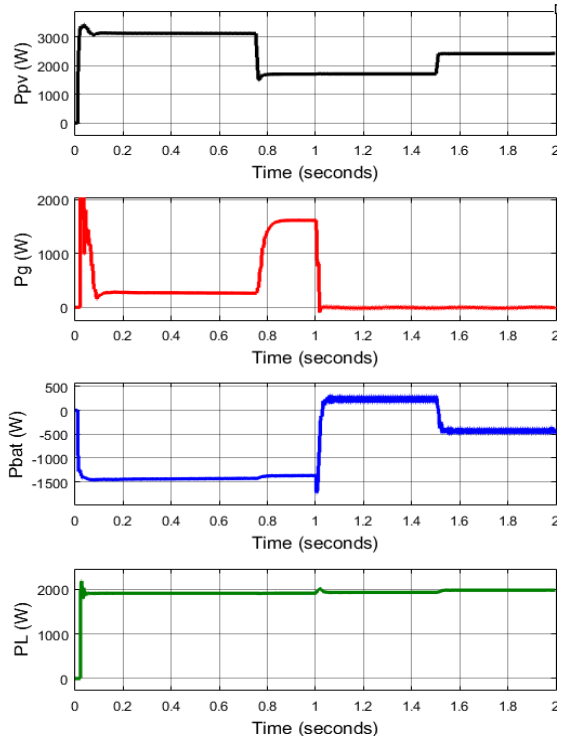

Figure 10: Active power of all modules

The figure 10 presents the graphs of the active powers of the modules connected in the system. It is observed that in any operating condition the residential load power of 2kW is always compensated irrespective of grid connection and PV power generation. Initially from 0-0.75sec when the PV power available is 3.1kW, the EV battery is charged with 1.5kW and the remaining 1.6kW is diverted to the residential load. With 0.1kW conversion loss the load receives 1.5kW PV power and 0.5kW grid power. At 0.75sec when the PV power drops to 1.8kW the deficit power to the residential load is compensated by the grid recorded to be 1.7kW. The 1.8kW of PV power compensates 1.5kW EV battery demand and 0.3kW is diverted to residential load. With grid disconnection at 1sec the EV battery provides 200W of deficit PV power to the residential load.

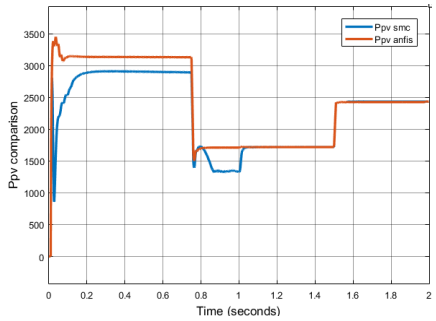

Figure 11: PV power comparison with SMC and ANFIS regulators

The figure 11 is the PV power comparison with SMC and ANFIS regulators in the full bridge converter controller. As observed in figure 11 the maximum power extraction is improved from 2.9kW to 3.1kW. And at 0.75sec the disturbances caused due to drop in irradiation is mitigated by the ANFIS regulator keeping the power stable, However, the power extraction from PV array after 0.75sec remains same.

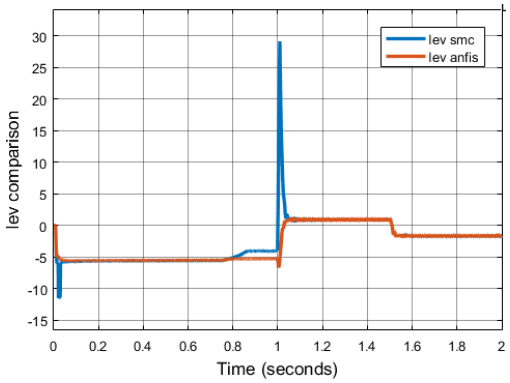

Figure 12: EV battery current comparison with SMC and ANFIS regulators

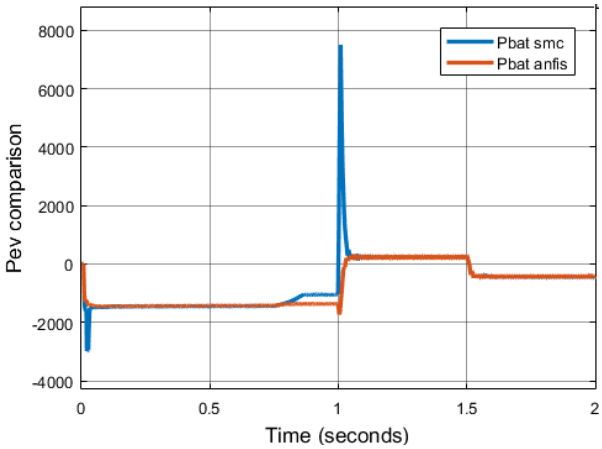

Figure 13: EV battery power comparison with SMC and ANFIS regulators

The figure 12 and 13 are the EV battery current and power respectively which have a reduced initial negative peak at 0sec and positive peak at 1sec during grid isolation. Due to the high damping of the SMC the peak overshoots during the transition are created which may damage the EV battery. The ANFIS regulator completely eliminates the overshoots in the current and power protecting the EV battery from the transitions on the grid.

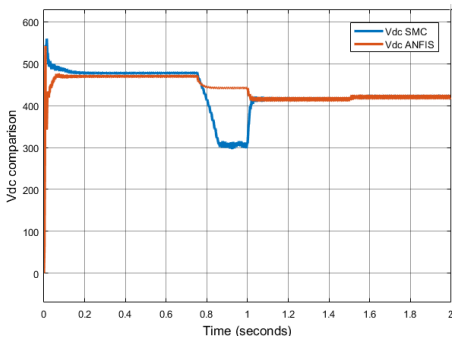

Figure 14: DC link voltage comparison with SMC and ANFIS regulators

The figure 14 shows the stability of the DC link voltage maintained by the ANFIS voltage regulator when there is a drop in solar irradiation and grid isolation conditions at 0.75 and 1sec. The DC voltage tend to maintain between 470 – 420V throughout the simulation in different operating conditions.

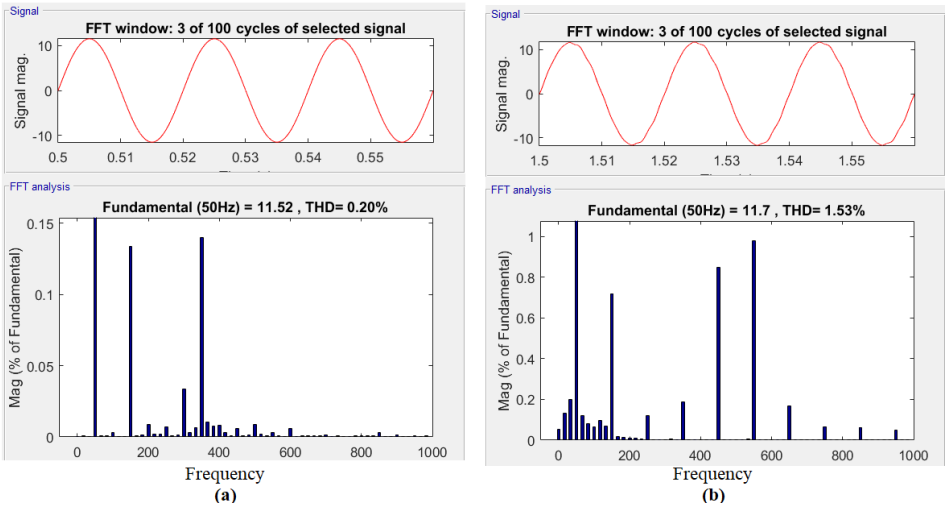

Figure 15: Load current THD (a) Grid connected mode (b) Grid isolation mode

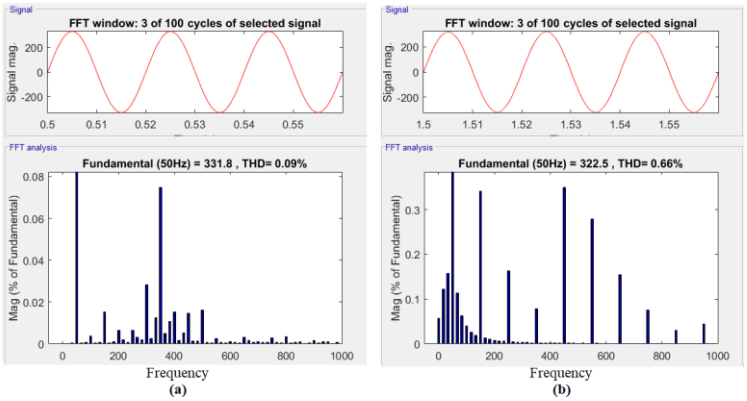

Figure 16: Load voltage THD (a) Grid connected mode (b) Grid isolation mode

The figure 15 and 16 are the THDs of the residential load current and voltage calculated by the FFT analysis tool during grid connected mode and grid isolation mode. In any given condition the

harmonics in the residential load voltage and current are recorded to be very low maintained below 2%. Even the residential load voltage magnitudes as per figure 16a and 16b are maintained at 331V and 322V indicating 230Vrms AC voltage maintained in both conditions. This shows the health of the system is stable irrespective of grid and PV power availability in the system where the load compensation is done by EV charger module.

5. CONCLUSION

The modeling and design of the proposed bidirectional SEPIC based multifunctional charger with grid interconnection and renewable power integration is implemented using Simulink blocks of MATLAB software. The bidirectional SEPIC converter is operated in both G2V and V2G modes as per the grid and PV power availability. The bidirectional SEPIC converter power direction is controlled by an EV charge control scheme controlling duty ratio of the switches Sev1 and Sev2. The direction of power flow of the full bridge converter is controlled a control scheme with feedback from DC link voltage, PV array voltage and current, load current, inverter voltage, grid voltage and current. In conventional full bridge control, a SMC based DC voltage regulator for the generation of reference current is used. This leads to heavy disturbances and peak overshoots in the DC link voltage and EV battery current respectively. As per the comparative results presented by the simulation graphs, it is observed that the DC link voltage is more stable and the overshoots in the EV battery current are completely eliminated when the full bridge controller is operated with ANFIS voltage regulator. Along with this the THDs of the load voltage and current at very low for any given condition of the simulation. These factors show the robustness and stability of the ANFIS over SMC regulator in the full bridge converter controller.

REFERENCES

[1] Egbue, O.; Long, S.; Samaranayake, V.A. Mass deployment of sustainable transportation: Evaluation of factors that influence electric vehicle adoption. *Clean Technol. Environ. Policy* 2017, *19*, 1927–1939.

[2] Alanazi, F. Electric Vehicles: Benefits, Challenges, and Potential Solutions for Widespread Adaptation. *Appl. Sci.* 2023, *13*, 6016. https://doi.org/10.3390/app13106016

[3] Castro, T.S.; de Souza, T.M.; Silveira, J.L. *Feasibility of Electric Vehicle: Electricity by Grid× Photovoltaic Energy*; Elsevier: Amsterdam, The Netherlands, 2017; Available online: https://www.sciencedirect.com/science/article/pii/S1364032116305895

[4] J. Meher and A. Gosh, "Comparative Study of DC/DC Bidirectional SEPIC Converter with Different Controllers," *2018 IEEE 8th Power India International Conference (PIICON)*, Kurukshetra, India, 2018, pp. 1-6, doi: 10.1109/POWERI.2018.8704363.

[5] A. Verma, B. Singh, A. Chandra and K. Al-Haddad, "An Implementation of Solar PV Array Based Multifunctional EV Charger," *2018 IEEE Transportation Electrification Conference and Expo (ITEC)*, Long Beach, CA, USA, 2018, pp. 531-536, doi: 10.1109/ITEC.2018.8450191.

[6] A. Verma, B. Singh, A. Chandra and K. Al-Haddad, "An Implementation of Solar PV Array Based Multifunctional EV Charger," in *IEEE Transactions on Industry Applications*, vol. 56, no. 4, pp. 4166-4178, July-Aug. 2020, doi: 10.1109/TIA.2020.2984742.

[7] M. Jamma, M. Akherraz and M. Barar, "ANFIS Based DC-Link Voltage Control of PWM Rectifier-Inverter System with Enhanced Dynamic Performance," *IECON 2018 - 44th Annual Conference of the IEEE Industrial Electronics Society*, Washington, DC, USA, 2018, pp. 2219-2224, doi: 10.1109/IECON.2018.8591620.

[8] A. Verma and B. Singh, "Multi-Objective Reconfigurable Three-Phase Off-Board Charger for EV," *IEEE Trans. Ind. App.*, vol. 55, no. 4, pp. 4192-4203, July-Aug. 2019.

[9] Y. Yang, Q. Jia, G. Deconinck, X. Guan, Z. Qiu and Z. Hu, "Distributed Coordination of EV Charging With Renewable Energy in a Microgrid of Buildings," *IEEE Trans. Smart Grid*, vol. 9, no. 6, pp. 6253-6264, 2018.

[10] Mahmud, Al Jaber & Mithun, Mehedi Hasan & Khan, Md & Faisal, Fahim & Nishat, Mirza & Hoque, Md. (2022). Optimal Control and Performance Enhancement of DC-DC Bidirectional SEPIC Converter. 0437-0443. 10.1109/UEMCON54665.2022.9965670.

[11] Lee H., Liang T. and Chen J. Design and Implementation of a Bidirectional SEPIC-Zeta DC-DC Converter *Proceedings of IEEE International Symposium on Circuits and Systems(ISCAS) (Melboume, June 2014)*

[12] Antchev, Hristo, Anton Andonov, and Dimitar Borisov. "Back-Up LED Lighting System with a Bidirectional SEPIC-ZETA Converter Based–A Computer Study." *2023 Eight Junior Conference on Lighting (Lighting)*. IEEE, 2023.

[13] H. Turker and S. Bacha, "Optimal Minimization of Plug-In Electric Vehicle Charging Cost With Vehicle-to-Home and Vehicle-to-Grid Concepts," *IEEE Trans. Veh. Tech.*., vol. 67, no. 11, pp. 10281-10292, Nov. 2018.

[14] M. Restrepo, J. Morris, M. Kazerani and C. A. Cañizares, "Modeling and Testing of a Bidirectional Smart Charger for Distribution System EV Integration," *IEEE Trans. Smart Grid*, vol. 9, no. 1, pp. 152-162, 2018.

[15] S. Taghizadeh, M. J. Hossain, J. Lu and M. Karimi-Ghartemani, "An Enhanced DC-Bus Voltage-Control Loop for Single-Phase Grid-Connected DC/AC Converters," *IEEE Trans. Power Electronics*, vol. 34, no. 6, pp. 5819-5829, June 2019.

[16] M. Furat and G. G. Cücü, "Design, Implementation, and Optimization of Sliding Mode Controller for Automatic Voltage Regulator System," in *IEEE Access*, vol. 10, pp. 55650-55674, 2022, doi: 10.1109/ACCESS.2022.3177621.

[17] Khan, S., Iqubal, N., Prasad, S. (2022). Voltage Regulator Using Sliding Mode Controller for Inverter Based Islanded Microgrid. In: Kumar, J., Tripathy, M., Jena, P. (eds) Control Applications in Modern Power Systems. Lecture Notes in Electrical Engineering, vol 870. Springer, Singapore. https://doi.org/10.1007/978-981-19-0193-5_12

[18] Zaky, M. S.: Design of multiple feedback control loops for a single-phase full-bridge Inverter based on stability considerations. *Electr. Power Compon. Syst.* **43**(20), 2325–2340 (2015)

[19] Soedibyo, Murdianto F.D, Suyanto, Mochamad A. and Ontoseno P. 2016 Modeling and simulation of mppt SEPIC combined bidirectional control invers KY converter using ANFIS in microgrid system *Indonesian Journal of Electrical Engineering and Computer Science* **1** 264-272 February

[20] Ghamari, S.M., Mollaee, H., Khavari, F.: Design of robust self-tuning regulator adaptive controller on single-phase full-bridge inverter. *IET Power Electron.* **13**(16), 3613–3626 (2020)

[21] Selami Balci, Kayabasi, A. & Yildiz, B. ANFIS Based Voltage Determination for Photovoltaic Systems According to the Specific Cell Parameters, and a Simulation for the Non-Isolated High Gain DC–DC Boost Converter Control Regard to Voltage Fluctuations. *Appl. Sol. Energy* **55**, 357–366 (2019). https://doi.org/10.3103/S0003701X19060100